



An apparatus for the determination of speeds of sound in fluids

Holger Gedanitz^{a,*}, María J. Dávila^a, Elmar Baumhögger^b, Roland Span^a

^a Lehrstuhl für Thermodynamik, Ruhr-Universität Bochum, D-44780 Bochum, Germany

^b Thermodynamik und Energietechnik (ThEt), Universität Paderborn, D-33098 Paderborn, Germany

ARTICLE INFO

Article history:

Received 17 June 2009

Received in revised form 30 October 2009

Accepted 2 November 2009

Available online 10 November 2009

Keywords:

Speed of sound

Pulse-echo technique

Water

Nitrogen

ABSTRACT

An apparatus for accurate measurements of the sound velocity in fluids is described, which is based on the pulse-echo technique, and operates up to 30 MPa in the temperature range between (250 and 350) K. The expanded uncertainties ($k = 2$) in the speed of sound measurements are 0.006%, 6 mK in the temperature, 2.1 hPa in the pressure up to 3 MPa, and 23.9 hPa above this value. Measurements of the speed of sound for nitrogen from (250 to 350) K and for water at temperatures between (303.15 and 323.15) K are presented at pressures up to 30 MPa to validate the new apparatus. The expanded overall uncertainty of the measurements on nitrogen and water were estimated to be 0.011% and 0.006%, respectively. The speed of sound of both fluids was compared with literature sources showing an excellent agreement among them, with relative deviations lower than 0.01% in nitrogen and 0.006% in water.

© 2009 Elsevier Ltd. All rights reserved.

1. Introduction

For numerous applications in technology and science, thermodynamic properties of pure fluids are required. Accurate properties are today available from fundamental equations of state [1]. The speed of sound plays a major role in establishing these equations. Because, in the limit of small amplitudes and low frequency the speed of sound is a thermodynamic state variable and connects the thermal and caloric properties [2]. Similar to pressure, temperature and density, the speed of sound is well accessible by experiment with high accuracy. But unlike thermal property data, speed of sound data is scarce, especially in the liquid state.

Over the last decades many techniques have been developed to determine the speed of sound in fluids. The spherical resonator has been used to obtain measurements with high accuracy in gases by Mehl and Moldover [3,4], Ewing *et al.* [5], Trusler and Zarari [6], and Benedetto *et al.* [7], whereas the pulse-echo technique is preferred for measuring the speed of sound in liquids and compressed gases at high pressure. Corresponding data were reported by Kortbeek *et al.* [8], Ye *et al.* [9], Wang and Nur [10], Zak *et al.* [11], Benedetto *et al.* [12], and Meier and Kabelac [13].

The aim of this work was the development of a new accurate instrument based on pulse-echo technique to determine the speed of sound in fluids in a temperature range between (250 and 350) K at pressures up to 30 MPa with high accuracy. Nitrogen and water were chosen as fluids to validate the technique, since they are commercially available in high purity, and since highly accurate litera-

ture sources and equations of state are available. Thus, the speed of sound for nitrogen was measured in a temperature range from (250 to 350) K at pressures between (20 and 30) MPa, whereas for water three isotherms were measured at (303, 313, and 323) K at pressures up to 30 MPa.

2. Experimental

2.1. Apparatus description

The speed of sound was determined by the pulse-echo technique. The ultrasonic sensor, [figure 1](#), is made of stainless steel 1.4571 and was subjected to a heat treatment to remove self-stresses from the manufacture process. The main pieces of the ultrasonic sensor are a piezoelectric quartz crystal mounted between two polished reflectors at (20 and 30) mm, respectively, and assembling these pieces by stainless steel screws. Both reflectors have conical cavities in the rear face to guarantee no echoes from the rear walls of the reflectors. The transducer is an X-cut crystal quartz of 15 mm diameter, which operates at its resonant frequency of 8 MHz, partially coated by gold main-electrodes with a diameter of 10 mm. Two clamps are used to connect the one electrode to ground potential *via* the stainless steel sensor and the second one to the high pressure electrical feed through by a copper wire. These clamps are connected to small areas outside of the main-electrode. Finally, the sensor has some openings to fill and to evacuate the fluid from the cell.

An Agilent 33220A function generator, whose time bases is connected to the frequency standard ELV FN 7000, was used to generate a sinusoidal burst signal to excite the piezoelectric transducer

* Corresponding author. Tel.: +49 (0) 234 32 26408.

E-mail address: Holger.Gedanitz@thermo.rub.de (H. Gedanitz).

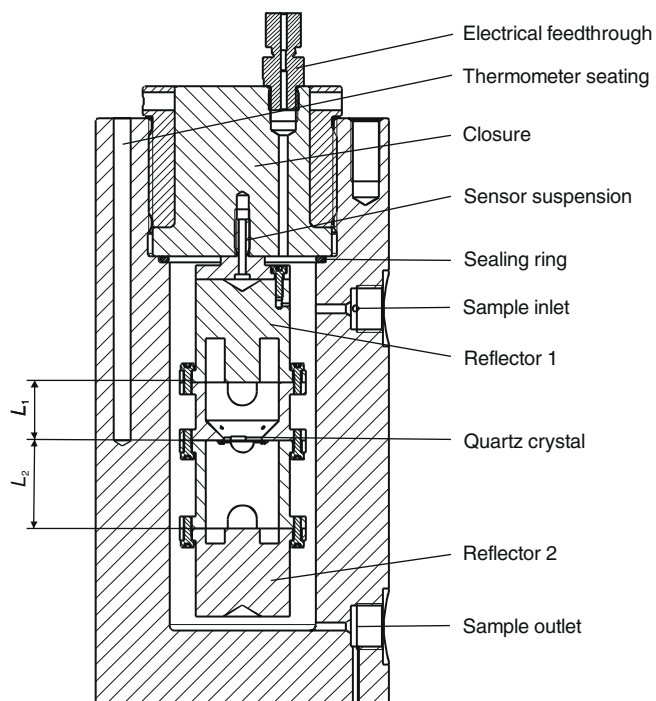


FIGURE 1. Cut through the speed of sound sensor and the pressure vessel.

and to trigger an Agilent Technologies MSO6032 digital storage oscilloscope. The function generator itself is triggered by the data acquisition computer with a repetition rate of 1 Hz, avoiding any overlap with echoes from previous excitations. The trigger signal is also used with a self-made circuit to control an electronic switch, which controls sending or receiving of signals from the oscilloscope to the piezoelectric crystal and *vice versa*. In addition, an Amplifier Research 1W1000B, which was required at the lowest temperatures in the calibration measurements, was connected between the switch and the oscilloscope to register the smallest amplitudes.

The pressure vessel, which contains the acoustic sensor, is made of stainless steel 1.4418, figure 1. It is connected to a coaxial cable,

which connects the ultrasonic cell to the electronic devices *via* a feed through which consists of a VCR fitting and a glass to metal sealing. At the operation frequency of 8 MHz it is necessary to match the wave impedance of the coaxial cable. Thus, an inductance is placed between the latter and the feed through. The inductance is located outside of the thermostat; thereby its value can be changed manually to obtain an optimal signal for different liquids.

The high pressure system (see figure 2) consists of two high pressure generators with a maximum pressure of 30 MPa; the first is connected to the nitrogen branch of the system, and the second one is connected to the sample fluid branch. Both branches are coupled by a differential pressure indicator Rosemount 3051S to communicate the pressure to the fluid branch. The changing of the zero point with pressure was removed by a preliminary calibration over the whole pressure range, whereas both sides of the differential transducer were filled with the same pressure. With this calibration the remaining uncertainty given by the manufacture is 1 hPa.

The pressure measurements were made by two pressure transducers, Paroscientific models 1000-500A and 1000-6K, being operative, respectively, up to (3 and 40) MPa. Both were checked against a pressure balance Degrange and Huot 5200. Moreover, a correction to the measured pressure was applied, taking into account the hydrostatic pressure differences from the location of the pressure transducers and the ultrasonic cell. The expanded uncertainty of the pressure measurements was estimated to be 2.1 hPa for pressures below 3 MPa and 23.9 hPa up to 30 MPa.

The pressure vessel was placed in a circulating liquid bath thermostat Fluke Corporation Hart Scientific 7060 to control the temperature of the acoustic sensor, which is filled with the sample fluid. As thermostating fluid a propylene glycol/water-mixture is used.

The temperature was measured by a Rosemount Aerospace 162CE Pt25 sensor with ITS-90 calibration in the height of the quartz crystal. The resistance of the thermometer was determined by a direct current bridge (TTI2, Isotech) using the internal resistant. The uncertainty of the temperature measuring consists of the uncertainty of the thermometer calibration (4 mK), the uncertainty of the measurements of the resistance ratio (2 mK), the stability of the temperature in the thermostat (1 mK, operating experience) and the homogeneity of the temperature field inside

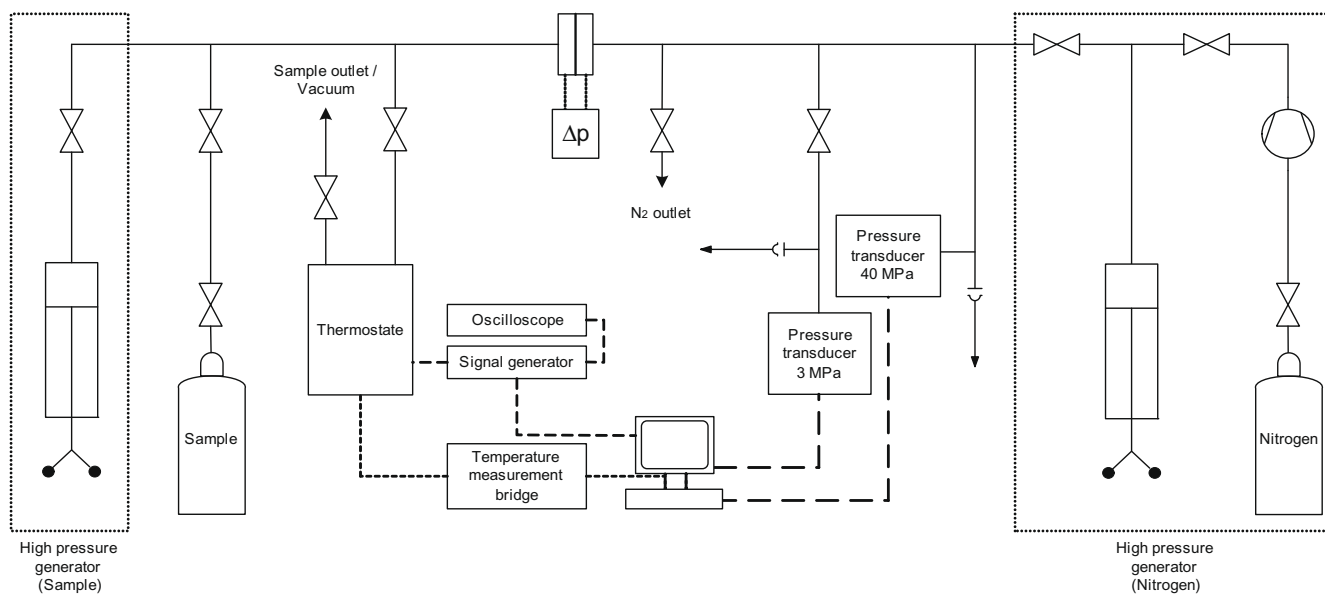


FIGURE 2. Schematic drawing of the filling pressure system (continuous lines), the electrical connections (dashed lines) and high pressure generators (pointed lines).

the pressure vessel (3 mK, estimated from a thermal budget). The distribution for all sources is assumed to be rectangular. Thus, the combined standard uncertainty of the temperature measurement is 3 mK over the temperature range of the instrument operation. The uncertainties in the course of this work were estimated following the recommended method by GUM [14].

2.2. Operation procedure

The quartz is electrically excited by a sinusoidal burst signal with around 60 cycles at its resonance frequency of 8 MHz, producing ultrasonic pulses that are propagated in both directions into the fluid. The transducer was used both as sender and receiver. The sound is reflected at the ends of the cell, which are located at $L_1 = 20$ mm and $L_2 = 30$ mm from the transducer, in order to make sure that the cell is suitable for measurements in the liquid and compressed gases speed of sound range. Thereby, the two echoes arrive at the quartz with a difference, Δt , in time, which is determined by a cancellation method [13]. The crystal is excited with a first burst signal and, after a time difference, with a second one, whereas the sign is reversed. The time difference between the two signals and the amplitude of the second signal are adjusted so, that the second echo of the first signal cancels the first echo of the second one. The adjusted time difference between the two excited signals is then equal to Δt , the time difference of the two echoes. For a complete cancellation the amplitude of the second burst must be reduced because the attenuation of the second signal, which travels the shorter path, is less than for the first signal traveling the longer path. The signal cancellation is monitored in the storage digital oscilloscope and the data are transferred to the acquisition computer software. The resolution in the time difference is less than $2 \cdot 10^{-10}$ s.

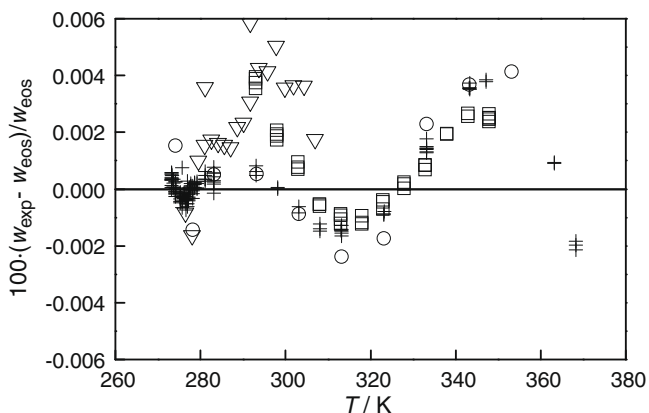


FIGURE 3. Relative deviations of the calibration measurements in water at ambient pressure from the IAPWS formulation [19] as a function of temperature: ○, This work; +, reference [16]; ▽, reference [17]; and, □, reference [18].

TABLE 1

Uncertainty budget for the acoustic length calibration.

Source of uncertainty	Value	Distribution	Divisor	Sensitivity coefficient	Standard uncertainty	Degree of freedom
Time measurement	$1 \cdot 10^{-5}$	Normal	1	1	$1 \cdot 10^{-5}$	∞
Calibration data	$1 \cdot 10^{-5}$	Normal	1	1	$1 \cdot 10^{-5}$	∞
Agreement of calibration and reference data	$1.5 \cdot 10^{-5}$	Normal	1	1	$1.5 \cdot 10^{-5}$	14
Repeatability	$1 \cdot 10^{-5}$	Normal	1	1	$1 \cdot 10^{-5}$	14
Pressure (0.1 MPa)	2.1 hPa	Normal	1	$\partial w / \partial p^a$	Negligible	∞
Temperature (274.15 K)	3 mK	Normal	1	$\partial w / \partial T^a$	$1 \cdot 10^{-5}$	∞
Combined standard uncertainty		Normal			$2.5 \cdot 10^{-5}$	>50

^a Calculated from reference [19].

The speed of sound in the fluid is calculated by the formulation:

$$w = 2(L_2 - L_1) / \Delta t. \quad (1)$$

The relation above is only applied to the ideal wave propagation, because diffraction effects have to be taken into account to evaluate the time differences between the ideal and real cases. Thus a correction has been applied to the measured time difference, following the method described by Harris [15], calculated for the source with Gaussian amplitude distribution. The correction is smaller than 0.01% in all experiments in this work. The relative uncertainty of the time difference measurement only consists of the uncertainty of the resolution of the time difference ($2 \cdot 10^{-5}$, rectangular distribution) and the uncertainty of the diffraction correction ($1 \cdot 10^{-5}$, rectangular distribution), since the uncertainty of the time base is negligible. Thus the quoted relative uncertainty of the time difference measurement is $1 \cdot 10^{-5}$, normal distribution.

The pathlength difference, ΔL , was obtained by calibration with purified water because of the availability of highly accurate speed of sound data, for example of the measurements obtained by Del Grosso and Mader [16], Kroebel and Mahrt [17], and Fujii and Masui [18], and of the fundamental equation of state available by Wagner and Pruss [19] (this equation was adopted as international standard for the properties of water and steam by the International Association for the Properties of Water and Steam, IAPWS, in 1995). The calibration measurements were carried out in a temperature range between (274.15 and 353.15) K, at 0.1 MPa. The calibration liquid, water in HPLC quality, was supplied by J.T. Baker and was degassed with ultrasound under vacuum before filling the evacuated high pressure system. The reproducibility of the measured speeds of sound was better than $1 \cdot 10^{-5}$.

The difference of the pathlength is determined from the equation (2), as a function of temperature, T , and pressure, p ,

$$\begin{aligned} \Delta L(T, p) &= 2(L_2 - L_1) \\ &= \Delta L(T_0, p_0) \cdot \left[1 + \alpha(T - T_0) + \frac{1}{E}(1 - 2\nu)(p - p_0) \right], \quad (2) \end{aligned}$$

where $\Delta L(T_0, p_0)$ is the acoustic pathlength at the reference points $p_0 = 0.1$ MPa and $T_0 = 293.15$ K; α , E , and ν are the linear thermal expansivity, elastic modulus, and the Poisson number of the stainless steel of the ultrasonic cell, respectively. The mechanical properties of the stainless steel sensor were obtained from reference [20]. The temperature dependences of the elastic modulus and the linear thermal expansivity are represented by first-order and fourth-order polynomials, while the Poisson number is considered independent of temperature. The change in the acoustic path length, which is given by the thermal expansion and compressibility of the quartz crystal as a function of pressure and temperature, is negligible. The contribution of the crystal to the acoustic length is negligible.

The acoustic pathlength of the sensor at the temperature and pressure of operation is determined by adjusting the pathlength at the reference points and the thermal expansion coefficient to obtain a similar deviation pattern from the IAPWS formulation as

TABLE 2
Uncertainty budget for the speed of sound measurement.

Source of uncertainty	Value	Distribution	Divisor	Sensitivity coefficient	Standard uncertainty	Degree of freedom
Length calibration	$2.5 \cdot 10^{-5}$	Normal	1	1	$2.5 \cdot 10^{-5}$	∞
Time measurement	$1 \cdot 10^{-5}$	Normal	1	1	$1 \cdot 10^{-5}$	∞
Expanded uncertainty		Normal ($k = 2$)			$6 \cdot 10^{-5}$	>50

the data of references [16,18], see figure 3. The relative agreement with the reference data is within $1.5 \cdot 10^{-5}$ over the whole temperature range of the calibration.

The uncertainty budget of the acoustic pathlength is given in table 1. The expanded uncertainty of the speed of sound measurements is $6 \cdot 10^{-5}$ and consists of the length calibration and the time measurements (see table 2).

3. Results and discussion

Water and nitrogen were chosen to validate the apparatus with respect to speed of sound measurements for liquids and compressed gases, respectively. Both fluids are usually available in high purity and were previously measured by many authors with high accuracy. Highly accurate fundamental equations of state have been developed by Wagner and Pruss [19] and Span *et al.* [21]. The speed of sound of compressed nitrogen was measured to test whether our ultrasonic cell agrees with the results of highly accurate spherical resonator technique, within our experimental uncertainty, in the pressure range where both methods overlap. Spherical resonators are commonly employed for speed of sound measurements in gases.

TABLE 3
Experimental speeds of sound u for water at pressures p and temperatures T .

T/K	p/MPa	$u/(\text{m} \cdot \text{s}^{-1})$
303.151	30.146	1559.693
303.150	25.038	1551.107
303.150	20.098	1542.820
303.150	15.130	1534.454
303.150	10.095	1525.978
303.150	5.051	1517.489
303.150	0.106	1509.135
313.150	30.168	1580.446
313.150	25.156	1571.970
313.150	20.133	1563.374
313.150	15.096	1554.749
313.151	10.102	1546.181
313.150	5.071	1537.492
313.151	0.109	1528.872
323.151	30.131	1595.322
323.151	25.069	1586.598
323.151	20.147	1578.057
323.151	15.095	1569.171
323.151	10.187	1560.483
323.151	5.173	1551.609
323.151	0.102	1542.553

TABLE 4
Uncertainty budget for water measurement.

Source of uncertainty	Value	Distribution	Divisor	Sensitivity coefficient	Standard uncertainty	Degree of freedom
Speed of sound measurement	$3 \cdot 10^{-5}$	Normal	1	1	$3 \cdot 10^{-5}$	∞
Repeatability	$1 \cdot 10^{-5}$	Normal	1	1	$1 \cdot 10^{-5}$	4
Pressure	23.9 hPa	Normal	1	$\partial w/\partial p^a$	Negligible	∞
Temperature	3 mK	Normal	1	$\partial w/\partial T^a$	$5 \cdot 10^{-6}$	∞
Expanded uncertainty		Normal ($k = 2$)			$6 \cdot 10^{-5}$	>50

^a Calculated from reference [19].

3.1. Liquid water under pressure

The speed of sound in water was determined for the three isotherms (303.15, 313.15, and 323.15) K, at pressures up to 30 MPa in steps of 5 MPa. The experimental results are given in table 3 and their quoted uncertainty is given in table 4 assuming that the contribution of impurities is negligible. The same water quality and the same filling procedure as for the calibration were used.

Several authors determined the speed of sound in water under pressure with high accuracies: Wilson [22], 0.05%; Barlow and Yazgan [23], 0.02%; Aleksandrov and Larkin [24], 0.02%; Aleksandrov and Kochetkov [25] 0.03%; Ye *et al.* [26], 0.06%; Fujii [27], 0.005%;

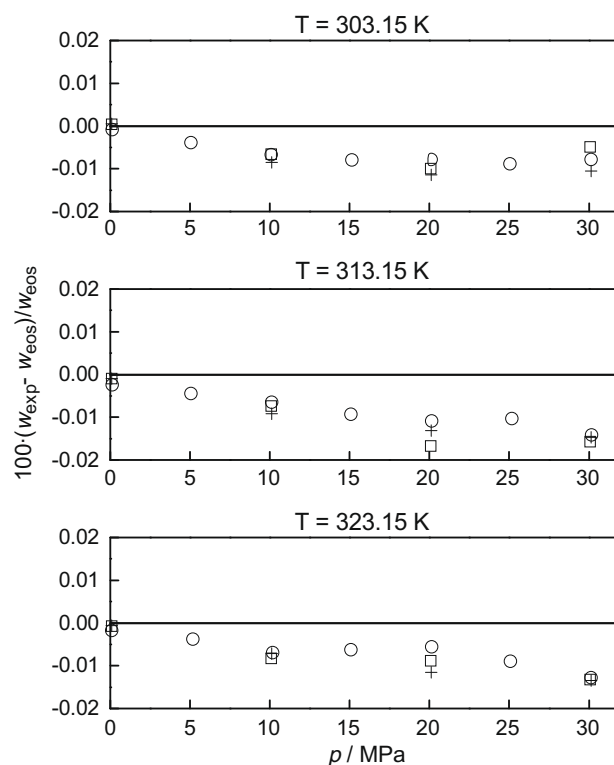


FIGURE 4. Relative deviations of the experimental speeds of sound u in water at (303.15, 313.15, and 323.15) K from the IAPWS formulation [19] as a function of pressure: \circ , This work; $+$, reference [13]; and \square , reference [27].

TABLE 5Experimental speeds of sound u for nitrogen at pressures p and temperatures T .

T/K	p/MPa	$u/(\text{m} \cdot \text{s}^{-1})$
249.997	29.944	480.255
249.998	27.655	462.799
249.998	25.461	446.075
249.998	22.571	424.318
249.998	20.061	405.959
275.000	30.156	480.548
275.000	27.555	463.238
275.000	25.048	446.737
275.000	22.551	430.655
275.000	20.063	415.185
299.999	30.080	483.653
299.999	27.506	468.426
299.999	25.029	454.007
299.999	22.557	439.965
299.998	20.033	426.134
350.000	30.129	497.896
350.000	27.528	485.109
350.000	25.025	473.012
350.000	22.529	461.236
350.000	20.040	449.851

Benedetto et al. [28], 0.05%; and Meier and Kabelac [13], 0.004%. The new experimental data were compared with those of Meier and Kabelac [13] and Fujii [27] because these are the data with the highest accuracies on the three isotherms.

For the three measured isotherms, figure 4 shows the percentage deviations of experimental results of this work, of the data by Fujii and by Meier and Kabelac from the IAPWS formulation [19] at pressures up to 30 MPa. The new speed of sound data agree with the IAPWS formulation within 0.014%, and with the two reference authors within 0.006% over the whole range of measurements. These results agree well with the uncertainty assessment given in table 4.

These measurements are not sufficient to validate the instrument. Because as a consequence of the calibration procedure with the same liquid, the variation of the speed of sound with pressure at the three isotherms was measured, but not the speed of sound itself. This raises the question if these good results are portable to other fluids and to temperatures outside of the calibration range. For this reason it was decided to measure nitrogen as another reference fluid.

3.2. Compressed nitrogen

The compressed nitrogen was supplied by Linde with 99.999% purity and was filled in the evacuated pressure system at room temperature. The experimental speed of sound data are given in table 5, for the four isotherms (250, 275, 300, and 350) K at pressures between (20 and 30) MPa in steps of 2.5 MPa. Below 20 MPa, measurements in nitrogen with the chosen acoustic pathlengths are not possible. The rise and fall times of the signals elongate with decreasing acoustic impedance (which decrease with pressure) of the fluid. Thus, a part of the first echo overlaps the region of cancellation. With another choice of the lengths,

TABLE 6

Uncertainty budget for nitrogen measurement.

Source of uncertainty	Value	Distribution	Divisor	Sensitivity coefficient	Standard uncertainty	Degree of freedom
Speed of sound measurement	$3 \cdot 10^{-5}$	Normal	1	1	$3 \cdot 10^{-5}$	∞
Repeatability	$1 \cdot 10^{-5}$	Normal	1	1	$1 \cdot 10^{-5}$	4
Pressure	23.9 hPa	Normal	1	$\partial w/\partial p^a$	$4.2 \cdot 10^{-5}$	∞
Temperature	3 mK	Normal	1	$\partial w/\partial T^a$	$3 \cdot 10^{-6}$	∞
Expanded uncertainty		Normal ($k=2$)			$1.1 \cdot 10^{-4}$	>50

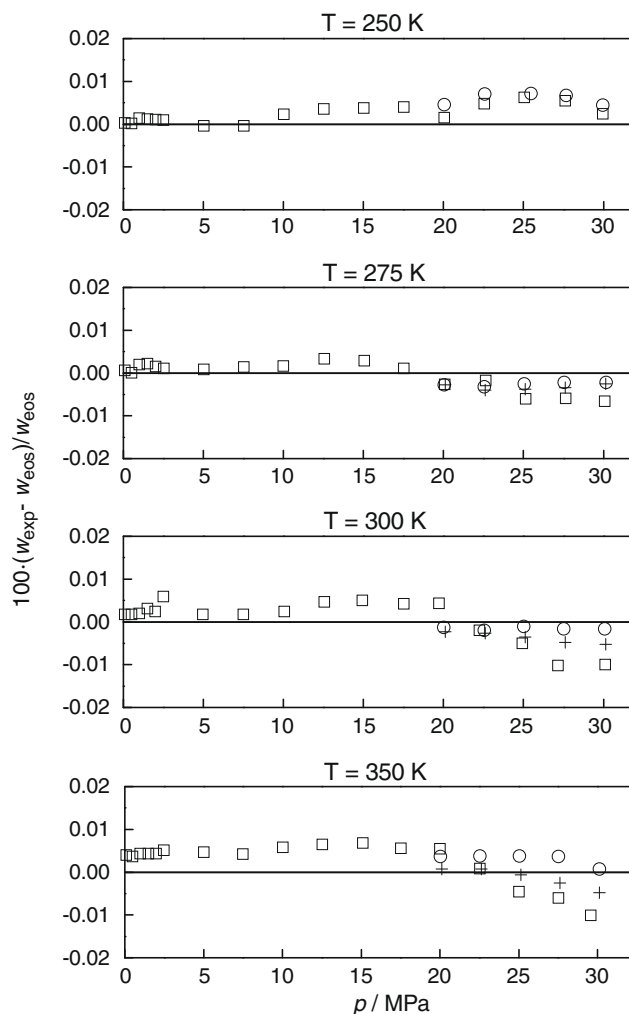
^a Calculated from reference [21].

FIGURE 5. Relative deviations of the experimental speeds of sound u in nitrogen at (250, 275, 300, and 350) K from the fundamental equation developed by Span *et al.* [21] as a function of pressure: \circ , This work; \square , reference [29]; and $+$, reference [31].

measurements below 20 MPa would be possible. For measurements at low pressures (<10 MPa) several changes might be required, e.g., an impedance matching layer between the quartz crystal and the nitrogen. The overall uncertainty of the speed of sound measurements in nitrogen is given in table 6. The contribution of impurities is considered negligible.

The sound speed in compressed nitrogen has been measured by several authors, but only some of them have obtained highly accurate data, as for example Costa Gomes and Trusler [29] with uncertainties from 0.001% to 0.01%; Kortbeek *et al.* [30], 0.02%; and Meier [31], 0.012%. The first two groups of authors have measured the speed of sound with a spherical resonator, while the last reference contains experimental data determined by the pulse-echo technique.

At the working frequency of 8 MHz the vibrational contribution to the effective heat capacity of nitrogen is completely absent. Thus, in contrast to water where the speed of sound is independent of the frequency up to 25 MHz [32], the experimental sound velocities of nitrogen were corrected using the equation given in reference [29] to the zero frequency value, which is related to other thermodynamic properties.

The new experimental data were compared with data from two literature sources. Figure 5 shows percentage deviations of speed of sound values determined in this work, together with the speed of sound data that were reported by Costa-Gomes and Trusler [29] and by Meier [31], from the fundamental equation of state by Span *et al.* [21]. Our experimental values agree with the reference equation of state within 0.01%, whereas the deviation to the data by Costa-Gomes and Trusler [29] and by Meier [31] is within 0.007% over the whole temperature and pressure range. Obviously, results measured with our new apparatus agree well with other highly accurate experimental data measured with spherical resonators and pulse-echo techniques.

Acknowledgements

The authors are grateful to Ministerio de Educación y Ciencia (Spain) for the financial support granted to María J. Dávila and to the Deutsche Forschungsgemeinschaft (DFG) for its financial support. Furthermore we are grateful to K. Meier and S. Kabelac for their support.

References

- [1] R. Span, Multiparameter Equations of State – An Accurate Source of Thermodynamic Property Data, Springer, Berlin, 2000.
- [2] J.P.M. Trusler, Physical Acoustic and Metrology of Fluids, Adam Hilger, 1991.
- [3] J.B. Mehl, M.R. Moldover, J. Chem. Phys. 74 (1981) 4062–4077.
- [4] J.B. Mehl, M.R. Moldover, J. Chem. Phys. 77 (1982) 455–465.
- [5] M.B. Ewing, A.R. H Goodwin, M.L. McGlashan, J.P.M. Trusler, J. Chem. Thermodyn. 19 (1987) 721–739.
- [6] J.P.M. Trusler, M. Zarari, J. Chem. Thermodyn. 24 (1992) 973–991.
- [7] G. Benedetto, R.M. Gavioso, R. Spagnolo, Rev. Nuevo Cimento 22 (1999) 1–42.
- [8] P.J. Kortbeek, M.J.P. Muringer, N.J. Trappeniers, S.N. Biswas, Rev. Sci. Instrum. 56 (1985) 1269–1273.
- [9] S. Ye, J. Alliez, B. Lagourette, H. Saint-Guirons, J. Arman, P. Xans, Rev. Phys. Appl. 25 (1990) 555–565.
- [10] Z.J. Wang, A.M. Nur, J. Acoust. Soc. Am. 89 (1991) 2725–2730.
- [11] A. Zak, M. Dzida, M. Zorebski, A. Ernst, Rev. Sci. Instrum. 71 (2000) 1756–1765.
- [12] G. Benedetto, R.M. Gavioso, P.A.G. Albo, S. Lago, D.M. Ripa, R. Spagnolo, Int. J. Thermophys. 26 (2005) 1667–1680.
- [13] K. Meier, S. Kabelac, Rev. Sci. Instrum. 77 (2006) 123903.
- [14] International Organisation for Standardization, ISO/IEC Guide 98 – 3: Uncertainty of Measurement – Part 3: Guide to the Expression of Uncertainty in Measurement (GUM 1995), Geneva, Switzerland, 2008.
- [15] G.R. Harris, J. Acoust. Soc. Am. 70 (1981) 10–20.
- [16] V.A. Del Grosso, C.W. Mader, J. Acoust. Soc. Am. 52 (1972) 1442–1446.
- [17] W. Kroebel, K.-H. Mahrt, Acustica 35 (1976) 154–164.
- [18] K. Fujii, R. Masui, J. Acoust. Soc. Am. 93 (1993) 276–282.
- [19] W. Wagner, A. Pruss, J. Chem. Phys. Ref. Data 31 (2002) 387–535.
- [20] Verein deutscher Eisenhüttenleute (Ed.): Stahl-Eisen-Werkstoffblätter: SEW 310 Tafel 43 9, Stahleisen: Düsseldorf, 1997.
- [21] R. Span, E.W. Lemmon, R.T. Jacobsen, W. Wagner, A. Yokozeki, J. Phys. Chem. Ref. Data 29 (2000) 1361–1433.
- [22] W.D. Wilson, J. Acoust. Soc. Am. 31 (1959) 1067–1072.
- [23] A.J. Barlow, E. Yazgan, Br. J. Appl. Phys. 18 (1967) 645–651.
- [24] A.A. Aleksandrov, D.K. Larkin, Teploenergetika 23 (1976) 75–78; A.A. Aleksandrov, D.K. Larkin, Therm. Eng. (Engl. Transl.) 23 (1976) 72.
- [25] A.A. Aleksandrov, A.I. Kochetkov, Teploenergetika 26 (1979) 65–66; A.A. Aleksandrov, A.I. Kochetkov, Therm. Eng. (Engl. Transl.) 26 (1979) 558–559.
- [26] S. Ye, J. Alliez, B. Lagourette, H. Saint-Guirons, J. Arman, P. Xans, Rev. Phys. Appl. 25 (1990) 555–565.
- [27] K. Fujii, Accurate measurements of the sound velocity in pure water under high pressure, in: 12th Symposium on Thermophysical Properties, Boulder, CO, USA, 1994.
- [28] G. Benedetto, R.M. Gavioso, P.A.G. Albo, S. Lago, D. Madonna Ripa, R. Spagnolo, Int. J. Thermophys. 26 (2005) 1667–1680.
- [29] M.F. Costa Gomes, J.P.M. Trusler, J. Chem. Thermodyn. 30 (1998) 527–534.
- [30] P.J. Kortbeek, N.J. Trappeniers, S.N. Biswas, Int. J. Thermophys. 9 (1988) 103–116.
- [31] K. Meier, The Pulse-echo Method for High Precision Measurements of the Speed of Sound in Fluids, Habilitation Thesis, University of Hamburg, 2006.
- [32] R. Barthel, A.W. Nolle, J. Acoust. Soc. Am. 24 (1952) 8–15.